Influence of Resolution of the Input Data on Distributed Generation Integration Studies

Ciontea, Catalin-Iosif; Sera, Dezso; Iov, Florin

Published in:
Proceedings of the 14th International Conference on Optimization of Electrical and Electronic Equipment, OPTIM 2014

DOI (link to publication from Publisher):
10.1109/OPTIM.2014.6851007

Publication date:
2014

Document Version
Accepted author manuscript, peer reviewed version

Influence of Resolution of the Input Data on Distributed Generation Integration Studies

Catalin I. Ciontea, Dezso Sera, Florin Iov
Department of Energy Technology, Aalborg University
cic@et.aau.dk, des@et.aau.dk, fi@et.aau.dk

***Abstract* – One of the main issues concerning large penetration of the renewable energy based generators on the distribution network is related to the voltage variations due to intermittent character of the solar irradiance and wind. The actual power quality standards provide only general information regarding the evaluation procedure of the voltage fluctuations and no directions regarding the sampling frequency of the data used. As a consequence, most of the studies neglect effect of the solar irradiance and wind speed in fast changing conditions on the utility grid. This work proposes a methodology to evaluate the voltage fluctuations into the low voltage distribution network caused by variable generation and reveals the influence of data resolution on the final results. A short review regarding the assessment of the voltage variations is presented in advance and an appropriate model of the power system is build, including the generating units that are capable to operate with high resolution input data. Real parameters for the components of the simulated system are used in order to obtain realistic results.**

I. INTRODUCTION

The interest in renewable energy is a result of the global concerns regarding pollution and increasing running cost of the power plants based on fossil fuel. As a consequence, more countries deployed new power plants based on renewable energy, with wind and photovoltaic (PV) representing the main focus [1]. Part of the new installed power is represented by residential generating units – at the end of 2013, only in Denmark 333 MW of PV were integrated within the low voltage (LV) distribution network [2].

More wind turbines (WT) and PV are expected to be installed in the LV networks, so new technical problems concerning the system operation arise [3]. Among the main issues caused by large penetration of the distributed generation (DG) in the LV network are the overvoltage at the end user and the voltage fluctuation due to the intermittent character of the renewable energy sources (RES) [2]. These shortcomings endanger normal operation of the devices and affect quality of the electric energy.

On the other hand, the increased share of the RES based DG allowed decommissioning of several conventional power plants based on fossil fuels and because most of the DG can sustain a short-circuit current of about 1 p.u. of the rated current, the electrical grid is weakened [4]. As result, the above mentioned technical issues due to integration of RES into the LV network are more pronounced because the weaker the network becomes, the more sensitive the voltage of the network is to the power fluctuations [4].

To overcome the drawbacks that characterize the large penetration of DG, some international standards define the system requirements and describe the general procedure to address the DG integration studies. Nevertheless, most of the research neglects effect of the fast changing conditions (rapid changes in solar irradiance or wind gusts) on the network behavior as the low sampling data are used and the final results may be inaccurate [6, 7]. Fig. 1 shows the difference between the same measured quantities but acquired with 3 different sampling times. Therefore, a study that uses low resolution data is unable to highlight the full extent of the impact of resource variability on the LV network. Moreover, the power quality standards do not define the maximum resolution of the data used in studies of the RES based DG.

This work aims to investigate the influence of resolution of the solar irradiance $G\ [W/m^2]$, ambient temperature $T_a\ [K]$ and wind speed $v\ [m/s]$ on a study concerning the impact of large penetration of the DG on the utility grid. Final objective of this paper is to propose a methodology for investigation of the power/voltage fluctuations into a LV network with high penetration level of DG and to indicate the adequate sampling time of the input data in order to obtain accurate results.

In order to achieve the proposed goals, this study follows the general outline for a steady-state DG integration research given in the IEEE-1547 standard and according to [5], the main steps of the work are:

- build the electrical model of the LV feeder
- build the DG models (PV system and WT)
- obtain the time profiles of the load and generation
- run the power flow simulation over a certain time
- based on the results, evaluate the voltage fluctuations

The novelty of the present study is that the parameters of a real LV network are used in the power flow simulations and

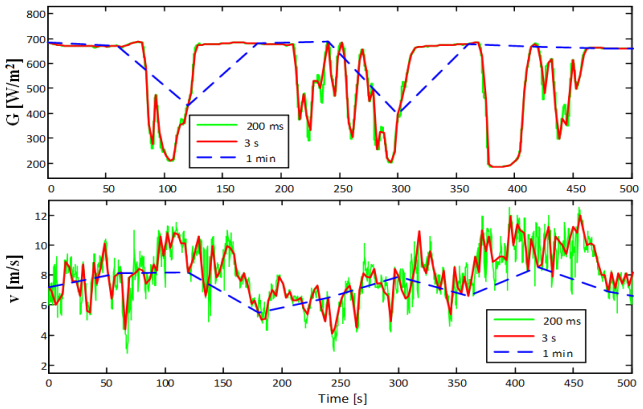

Fig. 1. One hour measured irradiance and wind speed data with 0.2 seconds, 3 seconds and 1 minute (interpolated) sampling time.

the input data of the models are obtained on-field with high sampling frequency. Matlab/Simulink software tool is used to model all components of the system and to implement the power flow algorithm as well. Models build are compatible with the high sampling frequency data and their output possess the same resolution as the input data. Consequently, effect of rapid changes in the solar irradiance or wind speed is considered and impact of the DG on the network voltage is appropriately evaluated during the fast changing conditions.

This paper is structured as follows. Section II reviews the assessment of the voltage variations, as presented in the power quality standards. In section III, the LV benchmark is described and the power flow method used in the present study is discussed. Section IV introduces the models of the PV systems and WT units that are connected to the LV feeder and a meteorological model that accounts for the effect of irradiance variations over a large area. Results of the power flow simulations are presented and discussed in Section V, followed by the conclusions, shown in Section VI.

II. ASSESSMENT OF THE VOLTAGE VARIATIONS

Power quality is assessed mainly by the voltage waveform quality at the Point of Common Coupling (PCC), according to the EN 50160 standard [8]. This paper focuses on the evaluation of the RMS voltage magnitude variations. The basic time interval for the measurements of the voltage is defined in the IEC-61000-4-30 standard as the 10 cycle time interval for a 50 Hz power system [9] and 3 aggregated time intervals are suggested:

- 3 second interval or very short variations (flicker)
- 10 minutes interval, used for short variations
- 2 hours interval, used for long variations [9]

However, only the 10 minutes time interval is used for evaluation of the voltage variations [9] and this is the time aggregation used to calculate the mean value and to check whether the voltage limits are exceeded [8]. Aggregation for each interval is performed using the voltage values from the previous aggregation and computing the RMS value [10], as presented in (1-2).

$$V_{RMS\_3s}(t_k) = \sqrt{\frac{1}{15}\sum_{i=k-15+1}^{k} V^2_{RMS\_200ms}(t_i)} \quad (1)$$

t_k *[s]* is the time sample at the end of the 3 seconds interval, t_i *[s]* is the time sample at the end of the 200 milliseconds interval, k is the index for the 3 seconds interval and i is the index for the 200 milliseconds interval.

$$V_{RMS\_10\min}(t_k) = \sqrt{\frac{1}{200}\sum_{i=k-200+1}^{k} V^2_{RMS\_3s}(t_i)} \quad (2)$$

t_k *[s]* is the time sample at the end of the 10 minutes interval, t_i *[s]* is the time sample at the end of the 3 seconds interval, k is the index for the 10 minutes interval and i is the index for the 3 seconds interval.

Reference [10] suggests a new method to evaluate the very short voltage variations in a time scale between the 3 seconds and the 10 minutes intervals. Accordingly, the very short variations are calculated in a 3 seconds or 10 minutes time scale. The "3 seconds" very short variations are calculated in (3), where V_{RMS_10min} is updated every 3 seconds.

$$\Delta V_{vs\_3s}(t_k) = V_{RMS\_3s}(t_k) - V_{RMS\_10\min}(t_k) \quad (3)$$

t_k *[s]* is the time sample at the end of the 3 seconds clock interval and k represents the index of the interval.

The "3 seconds" very short variations gives an information regarding the magnitude of the very short voltage variations as it represents the residue of the RMS voltage in a 3 second time scale with respect to the RMS voltage during the previous 10 minutes [10].

The "10 minutes" very short variations are calculated as the 10 minutes RMS value of the "3 seconds" very short variations in (4).

$$\Delta V_{vs\_10\min}(t_k) = \sqrt{\frac{1}{200}\sum_{i=k-200+1}^{k} \Delta V^2_{vs\_3s}(t_i)} \quad (4)$$

t_k *[s]* is time at the end of the 10 minutes interval, t_i *[s]* is time at the end of the 3 seconds interval, k is the index for the 10 minutes time interval and i is the index for the 3 seconds time interval.

Other quantities used in the scientific literature to quantify the voltage variations are the Voltage Fluctuation Index (VFI) and the Global Voltage Regulation (GVR). The VFI is the average change in the RMS voltage magnitude between two consecutive 200 milliseconds samples over the entire considered period [11] and is defined in (5).

$$VFI = \frac{\sum_{i=2}^{n} \left| V_{RMS\_200ms}(t_i) - V_{RMS\_200ms}(t_{i-1}) \right|}{n-1} \quad (5)$$

t_i *[s]* is the time sample at the end of the 200 milliseconds interval, i is the index of the 200 milliseconds interval and n is the total number of samples in the observation interval. In this paper, $n=18001$ for one hour voltage observation.

The GVR, given in (6), represents the RMS value of the voltage regulation (VR) in a number m of time intervals t_j *[s]*, where the VR is defined as the difference between the maximum and the minimum magnitude of the voltage for a single interval t_j [11, 12].

$$GVR = \sqrt{\frac{\sum_{j=1}^{m} \left[\max\left\{ V_{RMS\_200ms}(t_j) \right\} - \min\left\{ V_{RMS\_200ms}(t_j) \right\} \right]}{m}} \quad (6)$$

In this paper $m=36$, so the VR is evaluated every 100 seconds for one hour observation time of the voltage.

High values of the VFI and GVR suggest that the voltage profile has many high magnitude fluctuations. Instead, if the VFI value is low, but the GVR is high, it means that there are not too many short term fluctuations but some high peaks are present in the voltage profile. When the relative magnitude of

the VFI is high, it also entails a high GVR value, as both evaluate the voltage steps with the difference that the latter does it in a longer term than the former.

Equations (1-6) are based on measurement of the RMS voltage magnitude over a period of 200 milliseconds, according to the standards. This aspect drives to one of the requirements that the simulation model needs to fulfill: system components needs to refresh their output with the sufficient frequency in order to obtain the 200 milliseconds aggregation period for the RMS voltage.

III. LV Distribution Network

A. General Description and Load Profiles

In order to investigate the impact of the DG with high penetration level on the utility grid, the LV distribution network shown in Fig. 2 is studied. The considered network is derived from a real LV grid located in Brædstrup, Denmark and consists from 22 loads, 22 PV systems (one for each load), 3 WTs and 10 bus-bars. Each WT has a rated power of 10 kW, while each PV system is rated at 2 kWp. The aggregated load profiles for each bus are presented in Fig. 3.

The radial topology is selected for this study because it is characterized by higher voltage drops along the feeders compared to the loop or meshed types. Moreover, the radial topology is used intensive in the rural residential areas, where the disposable free space allows installation of the RES.

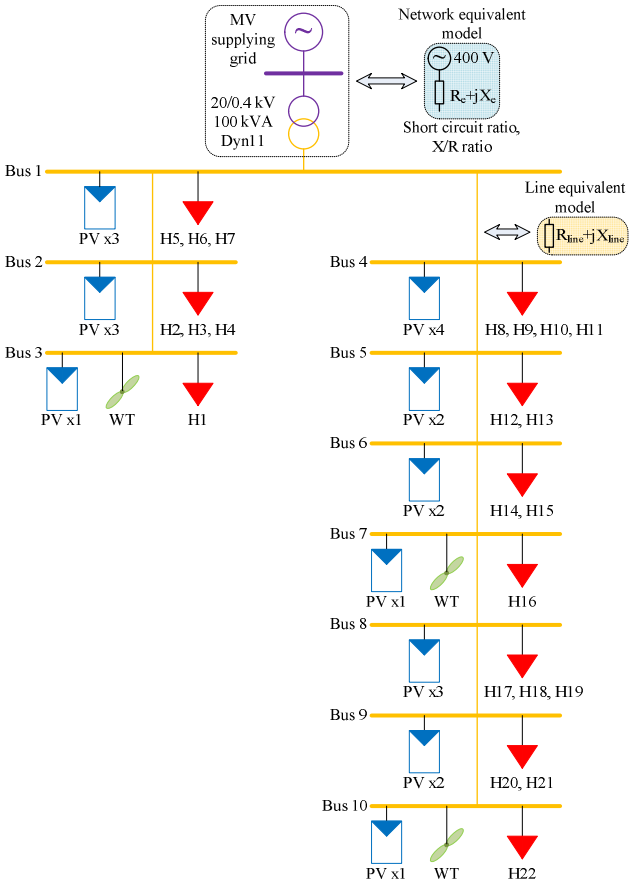

Fig. 2. LV distribution network and the equivalent simplified models of the electrical line, power transformer and utility grid

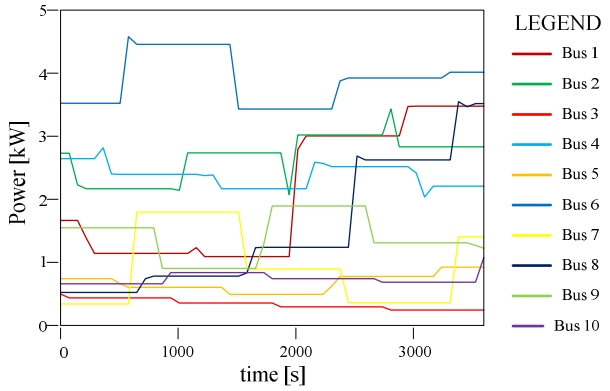

Fig. 3. Power consumption in each bus for one hour , 15 minutes resolution.

B. Supplying Grid and Power Transformer

The Medium Voltage (MV) supplying grid and the power transformer are modelled as an equivalent Thevenin circuit, shown in Fig. 2. According to [13], the equivalent resistance R_e and reactance X_e are calculated based on the parameters of the grid and power transformer in (7).

$$R_e + jX_e = R_{grid} + R_{traf} + j\left(X_{grid} + X_{traf}\right) \tag{7}$$

where R_{grid} $[\Omega]$, R_{traf} $[\Omega]$ and X_{grid} $[\Omega]$, X_{traf} $[\Omega]$ are the equivalent resistance and reactance respectively in the simplified model of the grid and transformer.

R_{grid} and X_{grid} are calculated in (8-9) as a function of the Short Circuit Ratio (SCR) and X/R ratio [13, 14].

$$R_{grid} = \frac{1}{SCR} \cdot \cos\left[\arctan\left(X/R\, ratio\right)\right] \tag{8}$$

$$X_{grid} = \frac{1}{SCR} \cdot \sin\left[\arctan\left(X/R\, ratio\right)\right] \tag{9}$$

Stiffness of the grid depends on the values of the SCR and X/R ratio. Weak grids have high X/R ratio and the SCR is less than 3, while the strong grids have low X/R ratio and the SCR is typically greater than 5 [15, 16].

R_{traf} $[\Omega]$ and X_{traf} $[\Omega]$ are calculated in (10-11) as function of the transformer parameters [14] given in TABLE I. Iron losses are neglected because power transformers are generally designed with high core permeability [14].

$$R_{trafo} = \frac{P_{Cu} \cdot V_2^2}{S_{rated}^2} \tag{10}$$

$$X_{trafo} = \frac{v_{shc} \cdot V_2^2}{S_{rated}} \tag{11}$$

V_2 $[V]$ is the secondary voltage, v_{sch} $[\%]$ is the short-circuit test voltage, P_{Cu} $[W]$ are the copper losses and S_{rated} $[VA]$ is the rated power of the transformer. As result, the equivalent impedance of the transformer is obtained in (12).

$$R_{traf} + jX_{traf} = 0.052 + j0.064 \tag{12}$$

TABLE I – PARAMETERS OF THE MV/LV POWER TRANSFORMER

Rated power [kVA]	Secondary voltage [V]	Short-circuit voltage [%]	Copper losses [kW]
100	400	4	3.25

C. Electrical Lines

Distribution lines consists from aluminum underground cables, used to connect different buses of the utility network and are symbolized with *Lx-y*, where *x* and *y* are the number of the starting, respective the ending bus-bar. Each cable is represented by an equivalent impedance denoted $R_{line}+jX_{line}$, as shown in Fig. 2. The real part of the impedance is the resistance and the imaginary part represents the reactance of the cable. The main electrical parameters of the lines are presented in TABLE II.

D. Power Flow Method

The power flow analysis is an important tool for the steady state analysis of the power system and it means calculation of the bus-bar voltages, of the voltage drops across the lines, power flow and power losses through the cables [14]. There are several iterative methods used in the power flow analysis or load flow, such as: Gauss-Seidel, Newton-Raphson and Fast Decoupled Load Flow [15].

In this paper, Gauss-Seidel algorithm is used because it provides adequate accuracy for small systems (low number of bus-bars) and requires low programming and computational effort [15]. Thus, its performances represent a trade-off between accuracy and complexity.

Purpose of the power flow analysis during the conducted study is to compute the bus-bar voltages based on the grid state and according to the active power that is injected or absorbed to each electric bus. According to this purpose and to the general objectives of this paper, the DG models need to generate the RMS value of the active power as a function of the environmental conditions, sampled with high frequency.

IV. Distributed Generation Modeling

A. Photovoltaic System

Structure of the PV model is represented in Fig. 4 and it consists from two main blocks: the PV generator and the average model of the inverter.

PV generators are composed from several PV cells that are connected in series/parallel and some by-pass diodes with

TABLE II – PARAMETERS OF THE LV DISTRIBUTION CABLES

Line	Resistance [mΩ]	Inductance [μH]	Reactance [mΩ]	Impedance R_l+jX_l
L1-2	72	14.99	4.71	72+j4.71
L2-3	46	9.58	3.01	46+j3.01
L1-4	25	12.96	4.07	25+j4.07
L4-5	24.6	8.82	2.77	24.6+j2.77
L5-6	17.7	6.33	1.99	17.7+j1.99
L6-7	88.5	28.71	9.02	88.5+j9.02
L7-8	135.4	37.24	11.7	135.4+j11.7
L 8-9	100	20.98	6.59	100+j6.59
L 9-10	79.2	16.49	5.18	79.2+j5.18

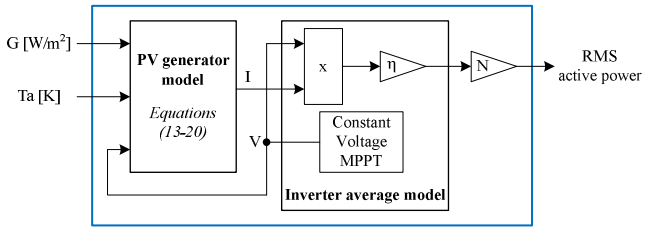

Fig. 4. Structure of the PV model – solar irradiance and ambient temperature are the input quantities and the RMS active power is the output parameter. It is assumed that the inverter efficiency is $\eta=0.95$ and the irradiance is constant over a single rooftop system (composed from *N* PV generators).

role in protection [17]. The current-voltage (I-V) and the power-voltage (P-V) curves characterizes behavior of the PV generator and due to their nonlinear nature, the PV generator outputs the maximum power for a single voltage – the maximum power point (MPP) [17]. Moreover, the MPP depends on the environmental conditions, so the operation point needs to be adjusted to reach the MPP, a process carried out by the Maximum Power Point Tracker (MPPT) [17].

This paper uses a simplified mathematical model to emulate the PV generator. This model is based on the main parameters of a real PV panel (given in datasheets), provides acceptable accuracy and is described in (13-15) [17].

$$I = I_{sc}\left[1 - C_1\left(e^{\frac{V}{C_2 V_{oc}}} - 1\right)\right] \tag{13}$$

$$C_1 = \left(1 - \frac{I_m}{I_{sc}}\right)e^{\frac{V}{C_2 V_{oc}}} \tag{14}$$

$$C_2 = \left(\frac{V_m}{V_{oc}} - 1\right)\left[\ln\left(1 - \frac{I_m}{I_{sc}}\right)\right]^{-1} \tag{15}$$

V *[V]* and I *[A]* are voltage and current of the PV generator and determine its operation point. V_{oc} *[V]*, V_m *[V]*, I_{sc} *[A]* and I_m *[A]* are the open circuit voltage, the MPP voltage, the short circuit current and the MPP current respectively, at different environmental conditions. Relations between these quantities and PV parameters at Standard Test Conditions (STC) are given in (16-19), according to [18].

$$V_{oc} = V'_{oc}\left[1 + c\left(T - T_{ref}\right) + \ln\left(1 + b\frac{G - G_{ref}}{G_{ref}}\right)\right] \tag{16}$$

$$V_m = V'_m\left[1 + c\left(T - T_{ref}\right) + \ln\left(1 + b\frac{G - G_{ref}}{G_{ref}}\right)\right] \tag{17}$$

$$I_{sc} = I'_{sc}\frac{G}{G_{ref}}\left[1 + a\left(T - T_{ref}\right)\right] \tag{18}$$

$$I_m = I'_m\frac{G}{G_{ref}}\left[1 + a\left(T - T_{ref}\right)\right] \tag{19}$$

V'_{oc} *[V]*, V'_m *[V]*, I'_{sc} *[A]*, I'_m *[A]* are parameters of the PV generator in STC and are given in datasheets. The rest of the parameters of the model are given in [18]: $a=0.00055\ K^{-1}$,

$b=0.5$, $c=0.00288\ K^{-1}$, $G_{ref}=1000\ W/m^2$ and $T_{ref}=298\ K$. $T\ [K]$ denotes temperature of the PV generator, which is related to the solar irradiance, Nominal Operating Cell Temperature (NOCT) and ambient temperature in (20), according to [19].

$$T = T_a + \frac{G}{800} NOCT - 293 \qquad (20)$$

The PV generator model is connected to the inverter average model, which emulates the power losses of a real PV inverter, multiplying the electric power (current-voltage product) with the efficiency η. It is assumed in this paper that the inverter efficiency is η=0.95, a typical value for a 2 kW inverter used in the residential PV applications [17]. Another important functionality of the PV inverter is the MPPT, which is also implemented in the model. Constant Voltage (CV) algorithm is selected to extract the maximum power because it offers acceptable performance for this study and is easy to implement it.

The CV method is based on the fact that the voltage changes logarithmically with the solar irradiance and the voltage at maximum power is a fixed percentage from the open circuit voltage for a wide range of irradiations [17]. As result, the MPP voltage is almost a constant percentage of the open circuit voltage, which is given by the manufacturers of the PV generator. However, this relation is not valid in partial shading conditions and operation of the CV algorithm is affected [17], but this aspect is irrelevant for this study.

To complete the PV system modeling, parameters in STC of the real PV generator used in this study are shown in TABLE III. Since a single PV generator is rated at 225 Wp, each rooftop PV system is composed from $N=9$ generators in order to obtain the desired power of about 2 kWp.

As result, the PV model generates an output power as a function of the solar irradiance and the ambient temperature, based on a mathematical model. Its implementation is simple, needs low computational power and the required parameters of the PV generator are provided by the manufacturer.

B. Wind Turbine

Structure of the WT model is illustrated in Fig. 5 and it consists from a look-up table and a 1st order transfer function that accounts for the mechanical inertia of the system. The look-up table expresses the generated power as a function of the wind speed. The typical time constant for a 10 kW unit is τ=1 second [20].

As result, model of the WT unit is simple and provides acceptable accuracy for the purpose of this study, providing an output power based on the input wind data.

C. Meteorological Model

The PV systems that are spread over a large area are not affected in the same time by a passing cloud, so their output power varies differently as the irradiance changes. As result, the power fluctuations of a PV system are smoothed by their geographical dispersion [21]. Therefore, a DG integration study needs to take into account these effects as the rooftop PV systems in the LV network are dispersed over a wide area and the irradiance data are not available for each site.

TABLE III – PARAMETERS OF THE PV GENERATOR (STREAM SE245M-30/E.b MODEL)

Rated power [Wp]	V'$_m$ [V]	V'$_{oc}$ [V]	I'$_m$ [A]	I'$_{sc}$ [A]	NOCT [K]
225	44.2	54.9	5.10	5.45	318

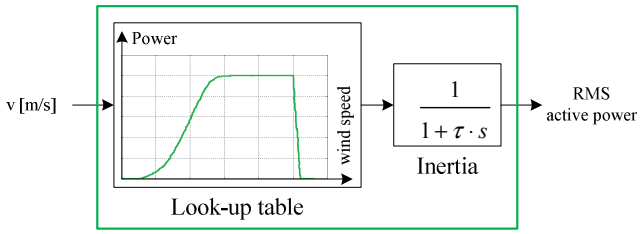

Fig. 5. Structure of the WT model – wind speed is the input quantity and the RMS active power is the output parameter. In simulations, the start-up speed is 3m/s, cut-off speed is 25 m/s and the nominal power is reached at 14 m/s.

A meteorological model is implemented and its operation is based on the following simplifying assumptions regarding irradiance variation in time or space:

- solar irradiance follows the same profile for each PV system, but these profiles are time shifted
- the time delay corresponding to two PV systems is a function of their location and movement (speed and direction) of the cloud that generates the irradiance variations over time

Accordingly, each PV system is affected in the same way, but time-delayed by fluctuations of the solar irradiance. As result, the purpose of the meteorological model is to compute the time delays between the instant when the first PV system is affected by the cloud and the times when the rest of the PV systems are perturbed.

Fig. 6 presents principle of the meteorological model for two PV systems affected by a passing cloud. If point A is perturbed at the moment $t=0$, then point B is affected by the same cloud after a time delay given in (21).

$$t_{delay} = \frac{d'}{v} = \frac{d \cdot \sin(\varphi - \theta)}{v} \qquad (21)$$

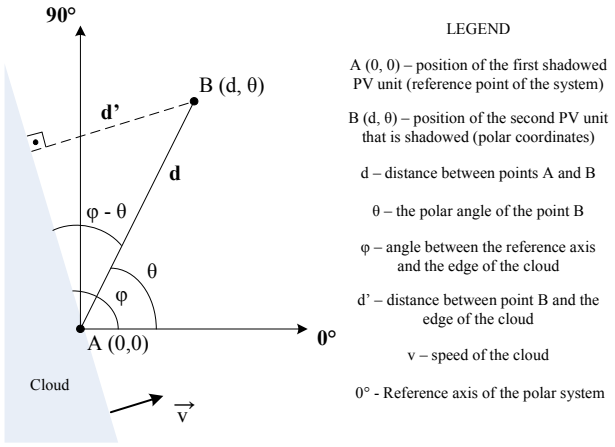

Fig. 6. Meteorological model. It is assumed that direction of the cloud and its edges are orthogonal and PV generators have the same spatial orientation.

This principle is applied to the case with 22 PV systems, thus the meteorological model used in the DG integration study based on high frequency input data is obtained. Polar coordinates of the PV systems are obtained from the maps of the town, while speed of the cloud is based on estimations. As result, the meteorological model outputs the time delays, as a function of the cloud speed and direction.

V. SIMULATION RESULTS

A. Simulation Input Data

The LV distribution network is defined, models of the DG units are successfully developed and the mathematical tools to evaluate the voltage variations are selected. Therefore, the prerequisite requirements for the proposed study are fulfilled and the general diagram of the simulation model is presented in Fig. 7. Components of the system are implemented using Matlab/Simulink software and the power flow is conducted for a period of one hour, using the real input data that are illustrated in Fig. 8, acquired at high sampling frequency.

For the MV supplying grid the following parameters are chosen: *SCR = 2* and *X/R ratio = 2* (weak grid). Speed of the cloud is set at *5m/s* and direction of the cloud over the area gives the time delays that are shown in TABLE IV.

B. Comparison of High Resolution Sampling Data with Low Resolution Data on Voltage Variations

This section aims to show the effect of data resolution on the voltage variations and for this purpose three cases are analyzed:

- 200 milliseconds resolution for the input data (case 1)
- 3 seconds resolution for the input data (case 2)
- 1 minute resolution for the input data (case 3)

Solar irradiance, ambient temperature and wind speed are

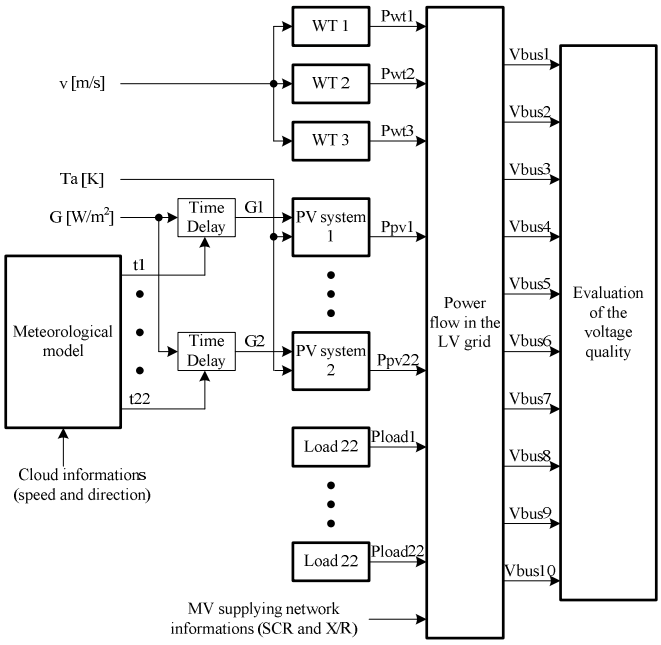

Fig. 7. Structure of the simulation model, including all components of the system and able to operate with different resolutions of the input data.

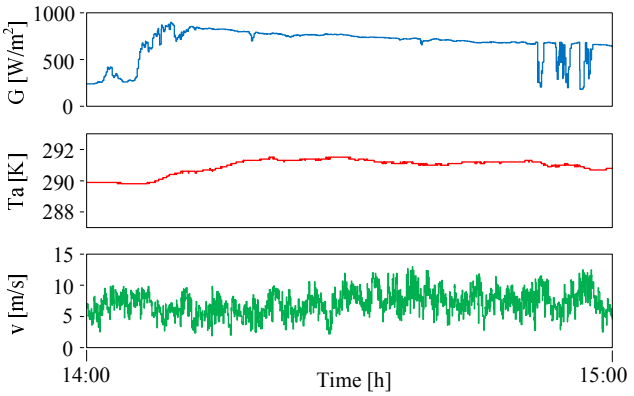

Fig. 8. Wind speed, ambient temperature and solar irradiance, acquired with 0.2 s sampling period (5 Hz sampling frequency) for 1 hour time-period

acquired at 200 milliseconds resolution and are down sampled at 3 seconds and 1 minute in order to obtain the input data for case 2 and 3. One hour simulation is accomplished for each of the scenarios, with the same given conditions, besides the resolution of the input data. Variations of the voltage are analyzed in the Bus 10 because of its location at the end of the feeder, where the voltage drops are the highest.

Fig. 9 illustrates the voltage profiles on Bus 10 for each of the considered resolutions of the input data for a period of 5 minutes, as the voltage profile for the entire duration of the simulation (one hour) is unintelligible in a picture. Voltage profile for cases 1 and 2 presents high short term variability, while case 3 is characterized by small variations on the short time scale, but with relatively large steps at each 60 seconds sample time.

Also, magnitude of the voltage is clearly different in case 3 compared to the cases 1 and 2 where no apparent difference on this parameter is depicted from the inspection of the RMS voltage plot. However, Fig. 9 does not allow a deep analysis of the voltage variations, but it only illustrates the apparent difference on the voltage profile for different resolutions of the input data within the selected time window.

TABLE IV – TIME DELAYS USED IN SIMULATIONS

PV system	PCC location	Time delay [s]	PV system	PCC location	Time delay [s]
1	Bus 3	67.7	12	Bus 5	35.1
2	Bus 2	63.2	13	Bus 5	34.1
3	Bus 2	64.0	14	Bus 6	31.5
4	Bus 2	59.5	15	Bus 6	38.0
5	Bus 1	55.1	16	Bus 7	42.7
6	Bus 1	56.5	17	Bus 8	37.2
7	Bus 1	50.5	18	Bus 8	30.3
8	Bus 4	45.4	19	Bus 8	24.6
9	Bus 4	47.2	20	Bus 9	15.2
10	Bus 4	40.5	21	Bus 9	10.7
11	Bus 4	43.9	22	Bus 10	0.0

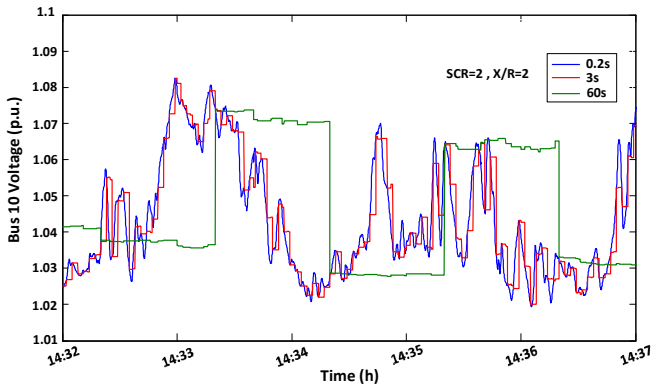

Fig. 9. Bus 10 voltage, 5 minutes time plot for different resolutions of the input data (solar irradiance, wind speed and ambient temperature).

Quantification of the voltage variations is made using the evaluation indicators suggested by different standards and discussed in Section II. Results for the voltage in Bus 10 are presented in TABLE V.

Difference of the mean value of 10 minutes aggregation of the RMS voltage between case 1 and case 2 is insignificant and compared to the case 3 is very small, thus resolution of the input data has little effect on the mean value of the RMS voltage aggregated over 10 minutes.

The mean value of the "10 minutes" very short variations suggest that in case 3, the voltage fluctuations are spread and have higher magnitude compared to the case 1 and 2. Fig. 10 reinforces this idea and presents the "10 minutes" very short variations and the "3 seconds" very short variations for different sampling periods of the input data. TABLE V and Fig. 10 shows that indicators of the very short variations of the voltage are similar for case 1 and case 2.

VFI and GVR indicators suggest that magnitude and number of the voltage variations is proportional with the resolution of the input data. A better picture of this idea is presented in Fig. 11, where the VFI and GVR are normalized using the value that corresponds to the case 1 ($3.126 \cdot 10^{-4}$ for VFI and 0.0424 for GVR) as the normalizing factor. Low resolution of the input data does not capture the full extent of the voltage fluctuations, as the normalized VFI and GVR presents high discrepancies between their magnitude at different cases.

Simulation results show that the high resolution input data can depict the voltage variations caused by fast changing conditions, while the low resolution input data are less adequate for this kind of studies, as the results are inaccurate in this case.

TABLE V – ASSESSMENT INDICATORS FOR VOLTAGE VARIATION IN BUS 10

Resolution of the input data	Mean value of V_{RMS_10min} [pu]	Mean value of ΔV_{vs_10min} [pu]	VFI	GVR
0.2 s	1.0298	0.01431	$3.126 \cdot 10^{-4}$	0.0424
3 s	1.0297	0.01455	$2.107 \cdot 10^{-4}$	0.0396
60 s	1.0303	0.01613	$0.3616 \cdot 10^{-4}$	0.0250

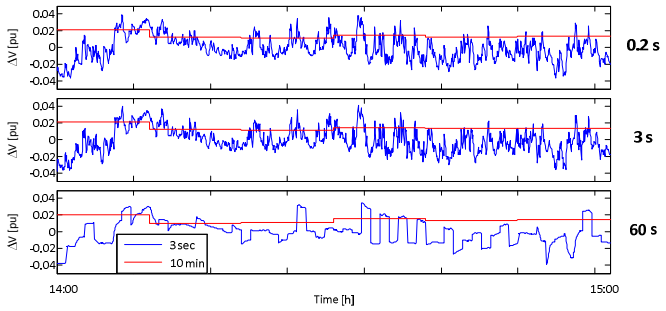

Fig. 10. Very short variations of the voltage, calculated in the time scale of 3 seconds and 10 minutes respectively for different resolutions of the data

VI. CONCLUSIONS

The DG integration studies are getting more important as the RES penetration level increases, the grid is weakened and the distribution system operator needs to ensure the quality of the supplying voltage. However, the results of these studies are highly dependent by the resolution of the input data, as this paper proves.

The grid operators and the standards should take this aspect into consideration, thus providing the adequate procedure to measure the amplitude of the RMS voltage variations.

In order to estimate correctly the voltage variations, based on this work, the following methodology is recommended:

- build the electrical model of the distribution network using accurate parameters of the components
- build the DG models and include their dispersion effect on the power output in order to avoid over estimation of the voltage fluctuations
- use adequate resolution to measure the input data (at least 3 seconds sampling time, depending on the assessment method, graphical or numerical)
- set low error for the power flow (0.1 % is used in this study) and run it for at least 1 hour simulation time
- evaluate the voltage variations using the mathematical tools provided in the standard (VFI and GVR provides good estimation in this study)
- compare the results obtained in different points of the network or in different networks to obtain the full picture of the fluctuations magnitude

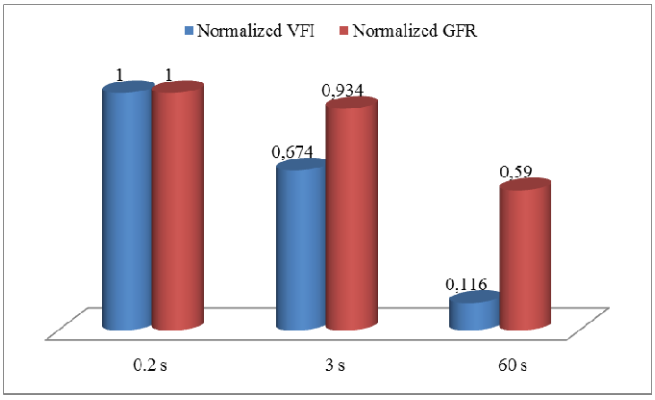

Fig. 11. Normalized VFI and GVR indicators of the voltage on Bus 10 for different resolutions of the input data

In practice, if the voltage is measured with low sampling frequency, the variations still exist, but people are aware of them to a lower extent. In simulations, if voltage is measured with high sampling frequency, but the input data of the models is acquired with low sampling frequency, the final results are misinterpreted.

In conclusion, the voltage fluctuations are proportional with the resolution of the input data used in the simulations, thus the actual power quality standards need to define the resolution limits for this type of studies.

ACKNOWLEDGMENT

The authors acknowledge the financial support from the European Union FP7 through the grant 318023 SmartC2Net and from the Forskel-Ease Wind.

REFERENCES

[1] EWEA, "Wind in power, 2012 European statistics", February 2013.

[2] Danfoss Solar Inverters A/S, "Voltage Control in low voltage networks by Photovoltaic Inverters-PVNET.dk", 2013.

[3] T. Ackermann, G. Andersson and L. Söder, "Distributed generation: a definition", *Electr. Power Syst. Res.*, vol. 57, pp. 195-204, 2001.

[4] R. Teodorescu, M. Liserre, P. Rodriguez, "Industrial/ PhD Course on Power Electronics for Renewable Systems - in Theory and Practice", October 2011, Department of Energy Technology, Aalborg University, Denmark.

[5] D. G. Photovoltaic and E. Storage, "IEEE Application Guide for IEEE Std 1547™, IEEE Standard for Interconnecting Distributed Resources with Electric Power Systems", 2009.

[6] J.L. Acosta, K. Combe, S.Z. Djokic, I. Hernando-Gil, "Performance Assessment of Micro and Small-Scale Wind Turbines in Urban Areas", *Systems Journal, IEEE*, vol. 6, pp. 152-163, 2012.

[7] J. Marcos, L. Marroyo, E. Lorenzo, D. Alvira and E. Izco, "Power output fluctuations in large scale PV plants: one year observations with one second resolution and a derived analytic model", *Prog. Photovoltaics Res. Appl.*, vol. 19, pp. 218-227, 2010.

[8] H. Markiewicz, A. Klajn, "Voltage Disturbances Standard EN 50160-Voltage Characteristics in Public Distribution Systems", 2004.

[9] E. IEC, "61000-4-30: Testing and measurement techniques–Power quality measurement methods", International Electrotechnical Commission Standard, 2003.

[10] M. Bollen, I.Y. Gu, "Characterization of voltage variations in the very-short time-scale", *IEEE Transactions on Power Delivery*, vol. 20, pp. 1198-1199, 2005.

[11] A. Nambiar, A. Kiprakis, A. Wallace, "Quantification of voltage fluctuations caused by a wave farm connected to weak, rural electricity networks", *14th International Conference in Harmonics and Quality of Power (ICHQP)*, 2010, pp. 1-8.

[12] M. Saied, "The global voltage regulation: a suggested measure for the supply quality in distribution networks", *International Journal of Electrical Power & Energy Systems*, vol. 23, pp. 427-434, 2001.

[13] S. Lundberg, "Electrical limiting factors for wind energy installations", Chalmers, Goteborg, Sweden, 2000.

[14] H. Saadat, “Power System Analysis”, Second Edition, McGraw Hill, New York, 2004.

[15] P. Kundur, “Power System Stability and Control”, McGraw Hill, New York, 1994.

[16] D. P. Kothari, K.C. Singal, R. Ranjan, “Renewable Energy Sources and Emerging Technologies”, Second Edition, Raj Press, New Delhi, 2011.

[17] R. Teodorescu, M. Liserre, P. Rodriguez, "Industrial/ PhD Course in Photovoltaic Power Systems - in Theory and Practice", October 2011, Department of Energy Technology, Aalborg University, Denmark.

[18] J. Xue, Z. Yin, B. Wu, J. Peng, "Design of PV array model based on EMTDC/PSCAD", *Power and Energy Engineering Conference*, APPEEC, 2009, pp. 1-5.

[19] J. D. Mondol, Y.G. Yohanis, M. Smyth, B. Norton, "Long-term validated simulation of a building integrated PV system", Solar Energy, vol. 78, pp. 163-176, 2005.

[20] J. Machowski, J.W. Bialek, J.R. Bumby, “Power System Dynamics”, John Wiley and Sons, 1997.

[21] J. Marcos, L. Marroyo, E. Lorenzo, M. García, "Smoothing of PV power fluctuations by geographical dispersion", *Prog. Photovoltaic Res. Appl.*, vol. 20, pp. 226-237, 2011.